Molecular and Conformational Determinants of Pituitary Adenylate Cyclase-Activating Polypeptide (PACAP) for Activation of the PAC1 Receptor

Steve Bourgault,[†,‡,§,||] David Vaudry,[‡,§,||] Isabelle Ségalas-Milazzo,[⊥,#,||] Laure Guilhaudis,[⊥,#,||] Alain Couvineau,[▽] Marc Laburthe,[▽] Hubert Vaudry,[‡,§,||] and Alain Fournier*[,†,§]

INRS—Institut Armand-Frappier, Institut National de la Recherche Scientifique, 531 boulevard des Prairies, Laval, Quebec H7V 1B7, Canada, INSERM U413, Laboratoire de Neuroendocrinologie Cellulaire et Moléculaire, Université de Rouen, 76821 Mont-Saint-Aignan, France, CNRS UMR 6014, Université de Rouen, 76821 Mont-Saint-Aignan, France, INSERM U773, Faculté de Médecine Xavier Bichat, 75870 Paris, France

Received March 7, 2009

PAC1 receptor is abundant in the CNS and plays an important role in neuronal survival. To identify the molecular determinants and the conformational components responsible for the activation of the PAC1 receptor, we performed a SAR study focusing on the N-terminal domain of its endogenous ligand, PACAP. This approach revealed that residues Asp^3 and Phe^6 are key elements of the pharmacophore of the PAC1 receptor. This study, supported by NMR structural analyses, suggests that the N-terminal tail of PACAP (residues 1 to 4) adopts a specific conformation similar to a turn when it activates the PAC1 receptor. Moreover, the integrity of the α-helix conformation observed at positions 5 to 7 appears crucial to allow the binding of PACAP. Characterization of analogues led to the identification of several superagonists, such as [Bip^6]PACAP27, and of a new potent PAC1 receptor antagonist, [Sar^4]PACAP38. The bioactive conformation inferred from this SAR study could constitute an appropriate molecular scaffold supporting the design of nonpeptidic PAC1 receptor agonists.

Introduction

Class B of G-protein-coupled receptors (GPCRs[a]) is a small family of GPCRs with low sequence homologies with other members of the GPCR superfamily.[1] These receptors regulate important endocrine and neuroendocrine functions and constitute attractive targets for the treatment of various diseases such as osteoporosis,[2] type II diabetes,[3] and migraine.[4] Class B GPCRs are endogenously activated by large peptide hormones. These peptide ligands include members of the secretin/glucagon/growth hormone-releasing hormone (GHRH) superfamily and members of the calcitonin family.[1] Class B receptors are often considered as difficult targets for drug development, as the identification of small molecules that can mimic the biological action of their large peptide ligands has been unsuccessful so far. Indeed, in contrast to class A GPCRs, nonpeptide ligands acting as potent agonists have not been identified and nonpeptide antagonists have only been documented for a small number of class B receptors.[4−6] The relatively large size of class B GPCRs ligands and the presence of a bulky N-terminal extracellular domain might explain the disparity in drug development between B and A GPCR families. A general mechanism for peptide interaction with class B GPCRs, known as the two-domain model, has emerged.[7] This highly accepted mechanism stipulates that the central and C-terminal segments of the peptide ligand bind to the N-terminal domain of the receptor and that the N-terminal region of the ligand interacts with the juxtamembrane domain of the receptor.[7] The interaction between the N-terminal segment of the peptide ligand and the core of the receptor is responsible for the activation of the receptor and the subsequent stimulation of intracellular signaling. This model is consistent with the structure−activity relationships (SAR) of class B GPCR ligands. Actually, C-terminal truncations decrease the binding affinity of these peptides, whereas truncations in their N-terminal segment suppress their biological activities.[8−10] The secondary structure of the members of the secretin/glucagon/GHRH superfamily in organic solvents or lipid micelles is mainly characterized by the presence of a stable α-helix generally consisting of the central and the C-terminal parts of the peptide.[11] On the other hand, N-terminal domains of these peptides are often disordered.[11] Because this region is responsible for the activation of the receptor, a better comprehension of the bioactive conformation of the N-terminal region of theses peptide ligands represents a key step in the rational design of potent nonpeptide agonists targeting class B GPCRs.

The PAC1 receptor, a class B GPCR, is pharmacologically attractive for treatment of various neurological insults such as stroke,[12] fetal alcoholism syndrome,[13] and drug-induced neurotoxicity.[14] Given that the activation of this receptor promotes neuronal survival,[12,13,15] the design of nonpeptide drugs that stimulate the PAC1 receptor constitutes a critical issue for the development of new therapeutic approaches targeting neurodegenerative diseases. Pituitary adenylate cyclase-activating polypep-

* To whom correspondence should be addressed. Phone: 1-450-687-5010. Fax: 1-450-686-5566. E-mail: alain.fournier@iaf.inrs.ca.
† INRS—Institut Armand-Frappier, Institut National de la Recherche Scientifique.
‡ INSERM U413, EA 4310, Laboratoire de Neuroendocrinologie Cellulaire et Moléculaire, Université de Rouen.
§ International Associated Laboratory Samuel de Champlain.
|| Institut Fédératif de Recherches Multidisciplinaires sur les Peptides (IFRMP23).
⊥ Université de Rouen, Equipe de Chimie Organique et de Biologie Structurale.
CNRS UMR 6014— COBRA.
▽ INSERM U773, Faculté de Médecine Xavier Bichat.

[a] Abbreviations: Aib, aminoisobutyric acid; BOP, benzotriazol-1-yl-oxy-*tris*(dimethylamino)-phosphonium hexafluorophosphate; Cha, cyclohexylalanine; Disc, 1,3-dihydro-2*H*-isoindole carboxylic acid; DPC, dodecylphosphocholine; Ind, Indoline-2-carboxylic acid; DSS, 2,2-dimethyl-2-silapentane-5-sulfonate; Fluo-4AM, Fluo-4 acetoxymethylester; Fmoc, 9-fluorenylmethyloxycarbonyl; GHRH, growth hormone-releasing hormone; GPCR, G-protein-coupled receptor; MALDI-TOF, matrix-assisted laser desorption time-of-flight; PACAP, pituitary adenylate cyclase-activating polypeptide; RP-HPLC, reverse-phase high performance liquid chromatography; SAR, structure−activity relationships; Tic, 1,2,3,4,-tetrahydroisoquinoline-3-carboxylic acid; Tiq, tetrahydroisoquinoline-1-carboxylic acid.

10.1021/jm900291j CCC: $40.75
Published on Web 05/04/2009

tide (PACAP), the endogenous ligand of the PAC1 receptor, exists in two C-terminally α-amidated isoforms, a 38-amino acid peptide (PACAP38) and its 27-residue N-terminal fragment (PACAP27).[16] As the other members of the secretin/glucagon/GHRH superfamily, the N-terminal domain of PACAP is essential for the activation of the PAC1 receptor.[10] For instance, removal of the first two residues of PACAP suppresses the PAC1 agonistic activity.[10] On the other hand, the PACAP(1−23) fragment acts as a complete PAC1 receptor agonist showing a decrease of its binding affinity.[17] When PACAP27 is bound to DPC-micelles, the conformation is characterized by an α-helix stretching from residues Ile^5 to Leu^{27} and a disordered N-terminal domain.[18] This helical conformation is also present when the antagonist PACAP(6−38) is bound to the N-terminal extracellular domain of the PAC1 receptor.[19] Notably, as determined by NMR, residues 3−7 seem to adopt an unusual β-coil structure made of consecutive type II′ (Asp^3-Gly^4-Ile^5-Phe^6) and type I β-turns (Gly^4-Ile^5-Phe^6-Thr^7) when the PACAP(1−21) fragment is bound to the PAC1 receptor.[18] Nevertheless, the bioactive conformation of the entire N-terminal domain inferred from SAR studies is still not available and the elucidation of this structure would certainly facilitate the rational design of nonpeptidic PAC1 agonists. Moreover, the key pharmacophores of the N-terminal domain of PACAP are still poorly characterized. Therefore, a SAR study focusing on the seven first residues of PACAP (His^1-Ser^2-Asp^3-Gly^4-Ile^5-Phe^6-Thr^7) was undertaken in order to identify the molecular determinants and the conformational components responsible for the activation of the PAC1 receptor. Residues His^1 to Ile^5 were selected for their biological significance while Phe^6 and Thr^7 were chosen because these two residues are highly conserved within the secretin/glucagon/GHRH superfamily.[20] As PACAP exists in two biologically active isoforms, our study was conducted on both PACAP38 and PACAP27 to evaluate the role of the 28−38 segment. The results suggest that the N-terminal domain of PACAP (residues 1−4) adopts a precise conformation when it activates the PAC1 receptor and that several chemical and structural determinants are essential to maintain the affinity and potency of PACAP.

Results and Discussion

Structural Study of PACAP27. To support the results of the present SAR study and to compare the structure of native PACAP with those of N-terminally modified analogues, the tridimensional conformation of PACAP27 in DPC environment was initially investigated. The structure adopted by peptide ligands in micelles is usually considered to reflect its membrane-bound conformation. When PACAP27 was bound to DPC-micelles, NOE connectivities characteristics of a helix conformation[21] ($d_{\alpha N}(i, i + 3)$ and $d_{\alpha N}(i, i + 4)$) were observed (Supporting Information). A total of 193 distance restraints (62 intraresidue, 62 sequential, 53 medium range, and 16 ambiguous) were deduced from NOE cross-peaks observed in the 100 ms NOEs spectrum and used for structure calculations. Analysis of the ϕ and Ψ angles revealed a good convergence for residues Ile^5-Leu^{27}. These residues were found in the energetically allowed ϕ/Ψ space and were located in the right-handed helix region of the Ramachandran plot (data not shown). In this region, all PACAP27 structures exhibited a similar helical backbone folding, as shown by the superimposition of the 92 final structures (Figure 1). A careful analysis of these structures revealed that the helix is extended from residues Ile^5 to Leu.^{27} Besides, the N-terminal segment 1−4 is mainly disordered (Figure 1). This conformation is consistent with the structure previously described by Inooka et al.[18] for PACAP27 in the same milieu.

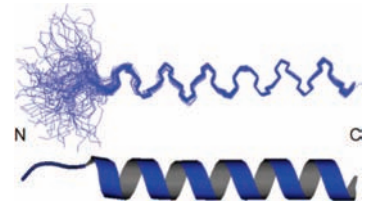

Figure 1. Backbone (N, Cα, and CO atoms) superimposition of 92 lowest energy conformers of PACAP27 between residues 5 and 27 and schematic ribbon representation of PACAP27 structure.

Table 1. Biological Data for Compounds **1**−**40**

no.	compd	IC_{50} (nM)[a]	EC_{50} (nM)[b]	E_{max} (%)[c]
1	PACAP27	8.3 ± 1.5	5.6 ± 1.1	102.2 ± 2.5
2	PACAP38	6.1 ± 1.1	2.1 ± 0.4	100.0 ± 1.9
3	[Ala^1]PACAP27	335 ± 132	174 ± 46	70.0 ± 3.9
4	[Ala^1]PACAP38	49.3 ± 13.5	11.0 ± 3.0	82.6 ± 3.7
5	[Ala^2]PACAP27	5.1 ± 1.4	6.8 ± 1.5	98.1 ± 3.0
6	[Ala^2]PACAP38	7.9 ± 1.4	5.1 ± 1.1	104.7 ± 3.3
7	[Ala^3]PACAP27	602 ± 164	538 ± 363	18.4 ± 4.6
8	[Ala^3]PACAP38	97.2 ± 27.7	(10 000)	64.1 ± 34.8
9	[Ala^4]PACAP27	9.1 ± 2.9	20.8 ± 2.0	104.9 ± 1.6
10	[Ala^4]PACAP38	9.84 ± 3.16	7.4 ± 2.2	90.2 ± 3.9
11	[Ala^5]PACAP27	60.7 ± 22.6	39.8 ± 3.8	99.2 ± 1.5
12	[Ala^5]PACAP38	34.4 ± 10.9	9.6 ± 2.1	88.3 ± 2.8
13	[Ala^6]PACAP27	1330 ± 341	462 ± 121	65.3 ± 4.2
14	[Ala^6]PACAP38	208 ± 62.4	17.3 ± 6.1	50.4 ± 3.2
15	[Ala^7]PACAP27	10.8 ± 1.5	8.75 ± 1.7	112.3 ± 3.1
16	[Ala^7]PACAP38	4.0 ± 1.3	0.8 ± 0.2	100.7 ± 3.3
17	[D-His^1]PACAP27	4.9 ± 1.6	15.2 ± 2.7	111.8 ± 3.0
18	[D-His^1]PACAP38	5.3 ± 1.7	2.9 ± 0.8	106.8 ± 4.0
19	[D-Ser^2]PACAP27	7.3 ± 2.2	8.4 ± 2.3	100.0 ± 3.7
20	[D-Ser^2]PACAP38	6.6 ± 2.2	4.1 ± 0.9	90.5 ± 2.2
21	[D-Asp^3]PACAP27	9.9 ± 4.5	18.6 ± 1.9	106.5 ± 1.7
22	[D-Asp^3]PACAP38	7.2 ± 2.4	7.6 ± 1.7	98.6 ± 3.4
23	[D-Ile^5]PACAP27	508 ± 113	199 ± 33	88.0 ± 3.0
24	[D-Ile^5]PACAP38	122 ± 35	16.0 ± 5.5	76.2 ± 4.2
25	[D-Phe^6]PACAP27	2310 ± 623	549 ± 109	37.6 ± 1.9
26	[D-Phe^6]PACAP38	951 ± 264	1840 ± 532	93.2 ± 8.6
27	[D-Thr^7]PACAP27	1410 ± 517	141 ± 36	72.8 ± 3.9
28	[D-Thr^7]PACAP38	119 ± 20.4	7.3 ± 1.7	63.3 ± 2.3
29	[N-Me-Ser^2]PACAP27	9.4 ± 2.9	48.8 ± 16.5	93.0 ± 6.1
30	[N-Me-Ser^2]PACAP38	9.1 ± 2.6	110 ± 25	87.7 ± 4.1
31	[N-Me-Asp^3]PACAP27	25.2 ± 10.2	418 ± 85	89.2 ± 5.9
32	[N-Me-Asp^3]PACAP38	10.4 ± 4.3	219 ± 33	92.5 ± 5.4
33	[Sar^4]PACAP27	308 ± 106	inactive[d]	
34	[Sar^4]PACAP38	97.0 ± 29	inactive[d]	
35	[N-Me-Ile^5]PACAP27	1770 ± 778	1810 ± 601	34.5 ± 5.0
36	[N-Me-Ile^5]PACAP38	158 ± 46	inactive[d]	
37	[N-Me-Phe^6]PACAP27	3150 ± 654	inactive[d]	
38	[N-Me-Phe^6]PACAP38	1280 ± 413	inactive[d]	
39	[N-Me-Thr^7]PACAP27	2040 ± 558	2120 ± 1130	35.4 ± 7.5
40	[N-Me-Thr^7]PACAP38	1010 ± 252	1010 ± 490	40.0 ± 6.6

[a] Concentration producing 50% of inhibition of specific binding of ^{125}I-Ac-PACAP27. [b] Concentration producing 50% of the maximal calcium mobilization. [c] Percentage of efficacy as compared to the maximal value obtained with PACAP38. [d] Inactive up to 1×10^{-6} M.

Alanine Scan. Initially, the seven first residues (His^1-Ser^2-Asp^3-Gly^4-Ile^5-Phe^6-Thr^7) of the N-terminal domain of both PACAP isoforms (**1**, **2**) were sequentially replaced by an alanine in order to determine the importance of each side-chain function for binding affinity and biological activity. Our results indicate that the carboxylic acid group of Asp^3 and the phenyl function of Phe^6 are crucial for activation of the PAC1 receptor as compounds **7**, **8**, **13**, and **14** are very weak partial agonists (Table 1; Figures 2 and 3). Compounds **3**, **4**, **11**, and **12** demonstrate a significant decrease of their binding affinities toward the PAC1 receptor, suggesting that the presence of an imidazole ring at position 1 as well as a large alkyl side chain on residue 5 facilitate the binding of the peptide. In particular, compound **3**

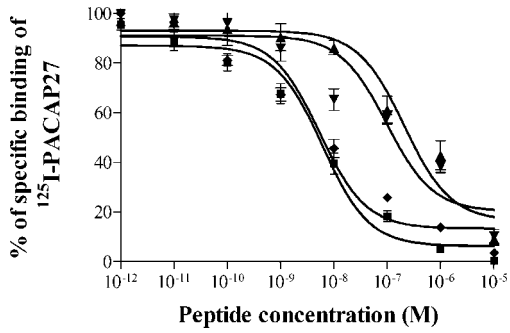

Figure 2. Inhibition of ^{125}I-Ac-PACAP27 binding to CHO cells stably transfected with the PAC1 receptor with increasing concentrations of PACAP38 (■), [Ala^6]PACAP38 (▲), [Sar^4]PACAP38 (▼), and [Bip^6]PACAP38 (◆). Data are expressed as a percentage of specific binding of ^{125}I-Ac-PACAP27 in the absence of competitive ligands. Data represent the mean ± SEM of 3−8 independent assays performed in triplicate.

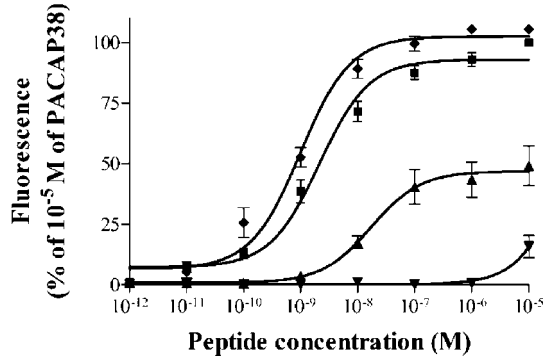

Figure 3. Representative concentration−response curves illustrating the effects of PACAP38 (■), [Ala^6]PACAP38 (▲), [Sar^4]PACAP38 (▼), and [Bip^6]PACAP38 (◆) on calcium mobilization in CHO cells stably transfected with the PAC1 receptor. Data are expressed as a percentage of the response (fluorescence intensity) obtained with 10^{-5} M PACAP38 added to the same experimental plate. Data represent the mean ± SEM of 4−10 independent assays performed in duplicate.

behaves as a weak partial agonist. On the other hand, analogues **5**, **6**, **15**, and **16** exhibit a similar potency to those of the native peptides, indicating that hydroxyl groups at positions 2 and 7 of PACAP are not involved in the activation of the PAC1 receptor. Interestingly, replacement of residue Thr^7 by Ala in the PACAP38 sequence led to the identification of a superagonist of the PAC1 receptor (**16**). In contrast, the PAC1 receptor was shown not to be tolerant to the incorporation of a bulky residue in position 2 of its ligand; [Arg^2]PACAP27 and [Phe^2]PACAP27 were weak agonists to induce adenylyl cyclase activation in AR 4-2J rat pancreatic acinar cells.[10] Finally, substitution of Gly^4 by Ala, a modification that reduces the flexibility of the peptide, did not affect significantly the binding affinity of both PACAP isoforms (**9**, **10**).

D-Amino Acid Scan. Second, the impact of the inversion of side-chain chirality on the biological activity of PACAP was explored. Our results revealed two distinct domains for the N-terminal segment of PACAP. Indeed, PAC1 receptor is tolerant to the substitution of residues His^1, Ser^2, and Asp^3 by their corresponding D-amino acid. For instance, compounds **17**−**22** are potent agonists with IC_{50} lower than 10 nM. On the other hand, incorporation of a D-amino acid at position 5, 6, or 7 was deleterious, reducing considerably the binding affinity of both PACAP isoforms. D-Amino acids are known to destabilize α-helix secondary structure.[22] Therefore, the lost of binding affinity observed for compounds **23**−**28** could be ascribed to a destabilizing effect on the helical conformation of the Ile^5-Thr^7 domain. As a matter of fact, the present structural data expose that, when **1** is bound to DPC micelles, a milieu that mimics the adjacent environment of the cellular membrane, the α-helix is extended from Ile^5 to Leu^{27} (Figure 1).

***N*-Methyl-Amino Acid Scan.** *N*-Methylation induces backbone conformational restriction and influences the orientation of the peptide bond.[23] Moreover, incorporation of a methyl group on the nitrogen atom of the amide bond blocks any potential hydrogen bond and gives some clues regarding the bioactive conformation of a peptide.[22,23] *N*-Methylation of Ser^2 and Asp^3 (**29**, **30**, **31**, **32**) did not reduce drastically the binding affinity of both PACAP isoforms. Nevertheless, these analogues showed a significant decrease of their potency to induce calcium mobilization in CHO cells transfected with the PAC1 receptor. On the other hand, *N*-methylation of PACAP at positions Ile^5, Phe^6, and Thr^7 (**35**−**40**) generated inactive compounds or very weak partial agonists with very low binding affinities (except for **36**), suggesting that PACAP is very sensitive to backbone restriction in this region. As shown in Figure 1, residues 5−7 adopt an α-helix conformation and the loss of affinity observed for compounds **35**−**40** might originate from a deleterious effect on this secondary structure. Substitution of Gly^4 by Sar (**33**, **34**) totally blocked the capacity of PACAP to activate the PAC1 receptor and decreased by 15- and 40-fold the affinity of PACAP38 and PACAP27, respectively. This result suggests that the nitrogen atom of Gly^4 could be involved in a hydrogen bond essential for activation of the PAC1 receptor.

Modifications at Positions 1, 3, or 6. Taking into account the results obtained from the Ala-Scan, the side chain of key residues (His^1, Asp^3, and Phe^6) were modified in order to obtain additional indications about the molecular requirements of the PAC1 receptor. The implication of the nitrogen atoms of His^1 in the activation of the PAC1 receptor was initially explored by incorporating methyl or acetyl groups (**41**−**46**). It appeared that the N-terminal amine function is not essential for biological activity as analogues **41** and **42** were potent agonists (Table 2). Similarly, methylation of the nitrogen atom at position 1 of the imidazole group did not affect significantly the potency of PACAP (**43**, **44**). Conversely, incorporation of a methyl group at position 3 of the imidazole ring of His^1 reduced drastically the efficacy of PACAP to activate the PAC1 receptor as analogues **45** and **46** behaved as weak partial agonists. Considering the efficacy reported for compound **4**, the inability of analogue **46** to properly activate the PAC1 receptor might come from steric hindrance produced by the methyl group rather than the blockage of a direct interaction between this specific nitrogen atom and the PAC1 receptor. Thus, methylation at position 3 of the His^1 imidazole ring could result in a failure of the N-terminal domain of PACAP to adopt its bioactive conformation or to penetrate efficiently into the activation pocket of the PAC1 receptor. In the same way, it has been shown that the substitution of His^1 with Phe reduced significantly the efficacy of PACAP27 to stimulate adenylyl cyclase activity of rat brain hippocampus membranes,[24] suggesting that the activation process of the PAC1 receptor is highly affected by the bulkiness of the aromatic group of residue at position 1 in the peptide ligand sequence.

Substitution of Asp^3 by Asn in PACAP27 reduced the peptide affinity without affecting its efficacy to stimulate calcium mobilization (**47**). Surprisingly, the same substitution applied to the 38-amino acid parent compound (**48**) partially abolished the activity of PACAP38 without reducing significantly its

Table 2. Biological Data for Compounds **40**−**81**

no.	compd	IC_{50} (nM)[a]	EC_{50} (nM)[b]	E_{max} (%)[c]
41	Ac-PACAP27	8.2 ± 1.8	9.7 ± 2.1	96.3 ± 3.1
42	Ac-PACAP38	5.7 ± 1.6	4.4 ± 1.2	91.1 ± 3.4
43	[His(1-Me)^1]PACAP27	15.6 ± 5.4	52.5 ± 10.3	96.9 ± 6.0
44	[His(1-Me)^1]PACAP38	7.5 ± 2.1	2.4 ± 0.9	87.6 ± 3.1
45	[His(3-Me)^1]PACAP27	21.6 ± 10.5	389 ± 157	31.9 ± 3.2
46	[His(3-Me)^1]PACAP38	11.3 ± 3.7	37.6 ± 14.1	18.2 ± 1.3
47	[Asn^3]PACAP27	284 ± 56	140 ± 14	91.2 ± 1.8
48	[Asn^3]PACAP38	9.2 ± 2.6	52.2 ± 23.5	22.1 ± 2.1
49	[Aad^3]PACAP27	818 ± 203	834 ± 212	29.3 ± 2.1
50	[Aad^3]PACAP38	12.5 ± 4.1	37.6 ± 14.1	18.2 ± 1.3
51	[Glu^3]PACAP27	10.6 ± 3.5	20.6 ± 5.0	90.5 ± 3.5
52	[Glu^3]PACAP38	7.0 ± 2.7	1.5 ± 0.4	87.6 ± 3.1
53	[Cha^6]PACAP27	11.0 ± 3.2	8.4 ± 1.6	105.4 ± 2.8
54	[Cha^6]PACAP38	6.6 ± 2.7	2.6 ± 0.7	97.7 ± 4.0
55	[Tyr^6]PACAP27	7.9 ± 2.8	7.7 ± 1.5	107.6 ± 2.8
56	[Tyr^6]PACAP38	6.7 ± 2.1	2.7 ± 0.4	99.4 ± 2.0
57	[Bip^6]PACAP27	4.5 ± 1.5	1.0 ± 0.3	103.8 ± 4.2
58	[Bip^6]PACAP38	5.4 ± 1.2	1.1 ± 0.4	105.1 ± 3.0
59	[Nal^6]PACAP27	6.5 ± 2.0	0.7 ± 0.2	110.5 ± 3.6
60	[Nal^6]PACAP38	5.0 ± 1.6	1.4 ± 0.5	105.9 ± 5.2
61	[Pro^2]PACAP27	7.8 ± 3.0	7.4 ± 1.6	94.2 ± 2.7
62	[Pro^2]PACAP38	8.5 ± 2.8	4.1 ± 0.7	89.3 ± 1.9
63	[Hyp^2]PACAP27	8.5 ± 2.9	2.3 ± 0.6	89.2 ± 2.8
64	[Hyp^2]PACAP38	8.6 ± 2.7	0.7 ± 0.2	94.0 ± 2.8
65	[D-Pro^2]PACAP27	268 ± 82	inactive[d]	
66	[D-Pro^2]PACAP38	76.3 ± 23.5	inactive[d]	
67	[Aib^2]PACAP27	9.5 ± 2.4	10.1 ± 1.7	103.8 ± 2.4
68	[Aib^2]PACAP38	7.2 ± 1.4	4.3 ± 1.0	94.8 ± 2.8
69	[Aib^4]PACAP27	51.4 ± 18.3	49.4 ± 12.2	90.2 ± 3.9
70	[Aib^4]PACAP38	9.2 ± 2.5	3.3 ± 1.1	84.0 ± 3.7
71	[γ-lactam^{4,5}]PACAP27	1980 ± 586	1030 ± 249	54.1 ± 3.8
72	[γ-lactam^{4,5}]PACAP38	775 ± 215	2480 ± 471	38.2 ± 2.4
73	[Ind^6]PACAP27	1940 ± 346	35.0 ± 4.9	72.0 ± 2.8
74	[Ind^6]PACAP38	not available		
75	[Tic^6]PACAP27	2170 ± 528	564 ± 82	65.9 ± 2.3
76	[Tic^6]PACAP38	1420 ± 220	4010 ± 2660	69.6 ± 24.6
77	[Tiq^6]PACAP27	2590 ± 808	inactive[d]	
78	[Tiq^6]PACAP38	1550 ± 515	inactive[d]	
79	[Disc^6]PACAP27	3590 ± 968	inactive[d]	
80	[Disc^6]PACAP38	1750 ± 470	inactive[d]	
81	PACAP(6−38)	56.7 ± 9.8	inactive[d]	

[a] Concentration producing 50% of inhibition of specific binding of ^{125}I-Ac-PACAP27. [b] Concentration producing 50% of the maximal calcium mobilization. [c] Percentage of efficacy as compared to the maximal value obtained with PACAP38. [d] Inactive up to 1×10^{-6} M.

binding affinity. The distance between the carboxylic acid function and the peptide backbone is also important for proper activation of the PAC1 receptor. For instance, elongation of the side chain of Asp^3 by two carbon atoms decreased drastically the efficacy of PACAP (**49**, **50**), suggesting that the activation pocket of the receptor might be very sensible to steric hindrance. Nonetheless, the PAC1 receptor was tolerant to the substitution of Asp^3 with Glu (**51**, **52**).

Substitution of Phe^6 with the nonaromatic cyclohexylalanine (Cha) residue did not alter significantly the potency of PACAP (**53**, **54**). In the same way, both PACAP isoforms were tolerant to the addition of a hydroxyl function at the para position of Phe^6 (**55**, **56**). Particularly, successive replacement of Phe^6 in PACAP27 with amino acids containing two aromatic rings increased significantly the potency, as [Bip^6]PACAP27 (**57**) and [Nal^6]PACAP27 (**59**) were 6- and 8-fold more potent than **1**, respectively. The equivalent modifications applied to the 38-amino acid isoform also appeared to slightly improve the potency of PACAP38 (**58**, **60**). However, these increases of potency were not statistically significant ($P > 0.05$). Taken together, these results suggest that the aromaticity of Phe^6 is not essential for the activation of the PAC1 receptor and that a bulky hydrophobic side chain at position 6 seems to increase the affinity and the potency of PACAP.

Local Conformational Constraints. Considering results from D- and *N*-methyl-scans, PACAP would be relatively

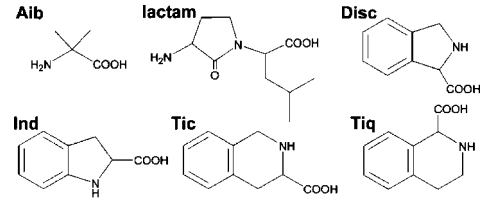

Figure 4. Chemical formulas of the different turn-inducing amino acid derivatives that were introduced in PACAP. Aib, aminoisobutyric acid; lactam, Gly-Val Freidinger γ-lactam; Disc, 1,3-dihydro-2*H*-isoindole carboxylic acid; Ind, indoline-2-carboxylic acid; Tic, 1,2,3,4,-tetrahydroisoquinoline-3-carboxylic acid; Tiq, tetrahydroisoquinoline-1-carboxylic acid.

tolerant to conformational modifications at position 2. Therefore, we applied structural restrictions at residue 2 in order to get further information about the bioactive conformation of the N-terminal segment. Substitution of Ser^2 with Pro, a turn-inducing amino acid, led to the identification of potent PAC1 agonists (**61**, **62**). Subsequent incorporation of a hydroxyl group at the γ position of the Pro^2 ring significantly increased the potency of the Pro-substituted analogues (**63**, **64**). In contrast, inversion of the chirality of this Pro residue at position 2 totally blocked the biological activity of PACAP but gave compounds (**65**, **66**) still able to bind to PAC1 receptor. These results suggest that the incorporation of Pro residue at position 2 induces specific conformational constraints, which are in agreement to the bioactive conformation of the N-terminal domain of PACAP. On the other hand, substitution of Ser^2 with D-Pro provoked structural restrictions that are not compatible with the activation of the PAC1 receptor. Ser^2 was also replaced with another turn-inducing amino acid, Aib (Figure 4), and analogues **67** and **68** showed similar potencies as their Pro^2-substituted counterparts.

It has been previously shown by NMR analysis that the segment 3−7 of PACAP21 adopts a unique conformation characterized by the presence of two consecutive β-turns (type II′ from Asp^3 to Phe^6 and type I from Gly^4 to Thr^7) when the peptide is bound to the PAC1 receptor.[18] To induce a β-turn involving residues 3 to 6, we substituted Gly^4 (position $i + 1$) with Aib (**69**, **70**) or the Gly^4-Ile^5 residues with a dipeptide Gly-Val Freidinger's γ-lactam (Figure 4) (**71**, **72**). Actually, γ-lactam conformational constraints are known to induce type II′ β-turn.[25] Nevertheless, our results demonstrated that PACAP is not tolerant to the rigidity produced by backbone cyclization at positions 4 and 5. Accordingly, compounds **71** and **72** were partial agonists with very low affinity toward the PAC1 receptor. In contrast, incorporation of Aib at position 4 did not affect drastically the potency of PACAP (**69**, **70**).

Bearing in mind that the hydrophobic side-chain of Phe^6 is essential for the biological activity of PACAP, we induced the hypothesized second β-turn (Gly^4 to Thr^7) by introducing several constrained turn-eliciting residues containing aromatic moieties (Ind, Tic, Tiq, Disc; Figure 4). None of the 7 analogues (**73**−**80**) showed satisfactory binding affinity ($IC_{50} > 1$ mM), suggesting that the α-helix found in the molecules spans up to positions 5−7 in order to favor the binding of PACAP to the PAC1 receptor. In addition, analogues **77**−**80** (Tiq^6 and Disc^6) were inactive, whereas **73** exhibited a moderate potency, indicating that the orientation of the phenyl group plays a favorable role for the activation of the PAC1 receptor.

Identification of Potent PAC1 Receptor Antagonists. All inactive peptides were initially tested for antagonistic activity using a fixed concentration of PACAP38 (1 μM) and 10 μM of inactive compounds (**33**, **34**, **36**, **37**, **38**, **65**, **66**, **74**, and **77**−**81**). For analogues that exhibited significant antagonistic properties

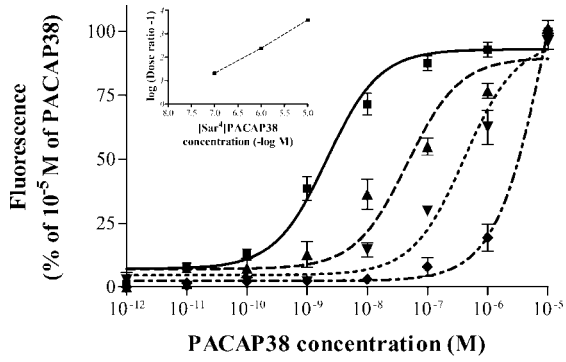

Figure 5. Effect of increasing concentrations of [Sar^4]PACAP38 on PACAP38-induced calcium mobilization in CHO cells stably transfected with the PAC1 receptor. The concentration response curves show the response to graded concentrations of PACAP38 in the absence (■) or in the presence of 0.1 (▲), 1 (▼), or 10 (◆) μM of [Sar^4]PACAP38. Data represent the mean ± SEM of 4−10 independent assays performed in duplicate. Inset: Schild plot revealed a slope of the Schild regression of −1.19. The *x*-axis intercept represents the pA_2 value according to Arunlakshana and Shild.[26]

Table 3. Antagonistic Activities of PACAP Analogues on PACAP-Induced Calcium Mobilization

no.	compds	pA_2[a]
34	[Sar^4]PACAP38	8.39
36	[Me-Ile^5]PACAP38	7.28
66	[D-Pro^2]PACAP38	7.45
81	PACAP(6−38)	7.96

[a] pA_2 values were obtained from concentrations ratios using 0.1, 1, and 10 μM of antagonists.

(**34**, **36**, **66**), the effects of increasing concentrations (0.1, 1, and 10 μM) of antagonists on PACAP38 calcium mobilization were analyzed and pA_2 values were estimated with the Schild plot (for example, see Figure 5).[26] The known PAC1 receptor antagonist, PACAP(6-38)[27] (**81**) was used as a reference molecule. The results showed that compounds **34**, **36**, and **66** were efficient PAC1 receptor antagonists (Table 3). Particularly, **34** was more potent than **81** to block calcium mobilization induced by PACAP38. This observation indicates that the presence of the N-terminal domain (residues 1−5) facilitates the inhibition of the binding of PACAP38 to the PAC1 receptor. Besides, the 28−38 segment was essential to confer a potent antagonistic activity because, even at a concentration of 10 μM, **33** was unable to reduce significantly the biological effect produced by 1 μM of **2** (data not shown).

Segment 28−38. PACAP exists in two biologically active isoforms constituted of 38 and 27 amino acids. Therefore, to evaluate the contribution of the C-terminal 28−38 segment on the binding affinity and potency of N-terminally modified PACAP analogues, our SAR studies was conducted with both isoforms. As a matter of fact, it has been previously shown that the C-terminal segment (28−38) facilitates the binding of PACAP to the PAC1 receptor.[10,24,27] Consistent with this notion, our results showed that chemical modifications applied to the N-terminal domain were generally less deleterious to PACAP38 analogues (even compound numbers) than to PACAP27 analogues (odd compound numbers). Indeed, IC_{50} obtained for the PACAP38 derivatives were generally lower than those measured for their PACAP27 counterparts. At the molecular level, PACAP27 derivatives exhibited a very similar capacity to activate the PAC1 receptor as their 38-residue parent compounds, as demonstrated by the relative similar maximal efficacy. Thus, the 28−38 segment seemed to facilitate the binding of PACAP to the PAC1 receptor without affecting considerably the efficacy of PACAP. Nevertheless, somewhat surprising data were obtained with analogues **47** and **48**. In fact, **47** was a complete agonist while its 38-residue counterpart (**48**) behaved as a partial agonist. This strongly suggested that the negative charge at position 3 was essential for the biological activity of PACAP38, while the 27-residue isoform was tolerant to the substitution of the carboxylic group with an amide function. It has previously been shown that the 28−38 segment had no impact on the conformation of the N-terminal domain, as PACAP38 and PACAP27 displayed similar N-terminal conformation.[28] For that reason, the difference in biological activity observed for [Asn^3]PACAP derivatives could not be ascribed to an influence of the 28−38 segment on the tridimensional structure of the N-terminal domain of PACAP. Therefore, the chemical determinant at position 3 responsible for the activation of the PAC1 receptor could be different for both PACAP isoforms. Nevertheless, this hypothesis will have to be tested.

Structural Study of PACAP27 Analogues. The N-terminal segment (1−4) of **1** is mainly disordered when the peptide is bound to DPC micelles (Figure 1). Nevertheless, as suggested by the present SAR study, the N-terminal 1−4 domain, which is essential for PAC1 activation, is believed to adopt a specific bioactive conformation. As a matter of fact, substitution of Ser^2 with Pro, a modification that causes a local conformational constraint, did not affect the potency of PACAP (**61**, **62**). In contrast, incorporation of a D-Pro at position 2 totally inhibited the biological activity of PACAP (**65**, **66**). Considering that the incorporation of a constrained residue such as Pro or D-Pro at position 2 probably stabilizes the conformation of the N-terminal domain, structural analysis of **61** and **65** were undertaken to obtain additional indications about the bioactive conformation of PACAP. The presence of a Pro residue is known to facilitate the cis−trans isomerization of peptide bond.[21] However, the observation of strong NOEs between αH(His^1) and δH(Pro^2) and the absence of "peak splitting" in TOCSY spectra showed that the proline residue at position 2 was predominantly in a trans conformation in both peptides. Both analogues displayed a similar tridimensional conformation as observed in PACAP27, i.e., an α-helix spanning from residues Ile^5 to Leu^{27} preceded by a less organized N-terminal domain. Nonetheless, as shown in Figure 6A, a careful analysis of **61** and **65** NOE connectivities in the N-terminal domain suggested the presence of a β-turn involving residues His^1 to Gly^4. In fact, both peptides exhibited a strong $d_{\alpha N}(i, i+1)$, a medium $d_{NN}(i+2, i+3)$ and a medium $d_{\alpha N}(i, i+2)$ NOEs, which are characteristic of type-II/II′ turns.[21] The ϕ and Ψ angles measured for the residue at position 3 were in agreement with these observations in both peptides. Mean ϕ and Ψ angles for the Asp^3 residue were characteristic of a type-II′ β-turn in **61** as well as in **65**.[29] In contrast, the ϕ and Ψ angles measured for the residue at position 2 in **61**, as well as in **65**, were not characteristic of any known β-turns.[29] Moreover, the distance between the Cα of His^1 (i) and Cα of Gly^4 ($i+3$) was superior to the 7 Å characteristic of a turn.[29] These findings can be ascribed to the fact that the residue i of this postulated β-turn is also the first residue of the peptide sequence. It is known that in solution the first residue of a peptide is generally in a fast moving state and, as a consequence, the chemical shift of its amine protons cannot be observed by NMR. This prevents any H-bond formation between residues 1 and 4 that could stabilize a β-turn and hinders the observation of additional NOE connectivities. Nevertheless, as illustrated in Figure 6B, the presence of a constrained residue at position 2, such as Pro or

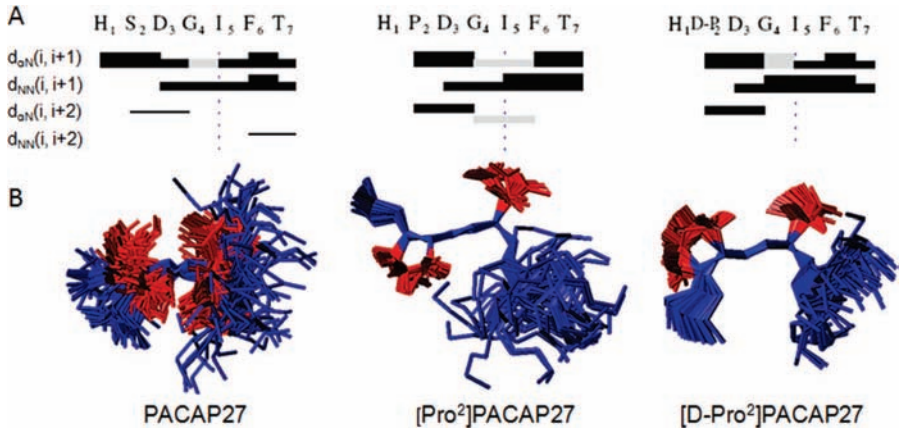

Figure 6. (A) Summary of NOE connectivities observed for the seven first residues of PACAP27, [Pro^2]PACAP27, and [D-Pro^2]PACAP27. The thickness of the lines reflects the intensity of the sequential NOE connectivities that is weak, medium, or strong. Complete summary of NOE connectivities for PACAP27, [Pro^2]PACAP27, and [D-Pro^2]PACAP27 are available as Supporting Information. (B) Superimposition between residues 2 and 3 of the 92, 55, and 87 lowest energy conformers of PACAP27, [Pro^2]PACAP27, and [D-Pro^2]PACAP27, respectively. Backbones (N, Cα, and CO atoms) from residues His^1 to Gly^4 are shown in blue, while the side chains of residues 2 and 3 are shown in red.

D-Pro, stabilized partially the conformation of the N-terminal domain of PACAP.

Proposed Bioactive Conformation. Taken together, our results suggest that the N-terminal domain (His^1-Ser^2-Asp^3-Gly^4-Ile^5-Phe^6-Thr^7) must adopt a precise and well-defined structure in order to favor the binding of PACAP to the PAC1 receptor and its further activation. As a matter of fact, the presence of a stable α-helix for segment 5−7 seems essential for the binding of PACAP. For instance, structural modifications known to destabilize an α-helix, and applied to positions 5−7 such as the incorporation of D- or *N*-methyl-amino acids, or the inclusion of conformational constraints, led to critical decreases of binding affinity. It was previously shown by NMR analysis that the segment 3−7 of PACAP(1-21) displays an unusual β-coil involving two consecutive β-turns.[18] Taking into account the data from the present SAR study, this unique structure observed by Inooka et al.[18] might result from a conformational change that occurs at the binding step and that is closely linked to the integrity of the α-helix, a crucial structure for the initial docking of PACAP to the PAC1 receptor.

The segment 1−4, which is essential for the activation of the PAC1 receptor, is disordered when PACAP27 is bound to DPC-micelles (Figure 1). Nevertheless, several indications suggest that this short N-terminal tail is susceptible to adopt a specific bioactive conformation similar to a turn. First, the empirical method of Chou and Fasman[30] predicts a β-turn for the sequence His-Ser-Asp-Gly. Moreover, His, Ser, Asp, and Gly exhibit a significant preference to be located at positions *i*, $i + 1$, $i + 2$, and $i + 3$ of a β-turn, respectively.[29−31] Second, replacement of residues His^1, Ser^2, and Asp^3 with their corresponding D-amino acids did not affect the potency of PACAP. In this respect, it is known that D-amino acids can stabilize turn conformation.[22,32] Third, incorporation of turn-promoting residues such as Pro, Hyp, or Aib at position 2 resulted in the production of potent agonists. Particularly, Pro and Aib are well-known to stabilize β-turn when they are located at position $i + 1$.[31,33,34] Fourth, NOESY spectrum of the constrained potent agonist, **61**, exhibited NOE connectivities characteristic of a β-turn[21] involving residues His^1 to Gly^4. For instance, a medium $d_{\alpha N}$ (i, $i + 2$) NOE connectivity, implicating residues Pro^2 and Gly^4, was observed (Figure 6A). Fifth, substitution of Gly^4, the residue $i + 3$ of the postulated turn, with Sar, resulted in incapability of PACAP to activate the PAC1 receptor. The incorporation of a methyl group on the nitrogen atom of the residue at position $i + 3$ of a β-turn blocks the formation of a hydrogen bond involving C−O(i) and N−H($i + 3$). Therefore, the fact that **34** is acting as a potent PAC1 antagonist could be associated to an inability of the N-terminal segment 1−4 to adopt a β-turn-like conformation. Finally, the low efficacy observed with the **45** and **46** derivatives is also compatible with the concept of a turn-like conformation involving residues His^1 to Gly^4. As mentioned above, the failure of compounds **45** and **46** to activate efficiently the PAC1 receptor is mainly attributed to steric hindrance produced by the methyl moiety. This methyl group located at position 3 of the imidazole ring seems to block the formation of the bioactive structure of the N-terminal domain obtained upon binding to the receptor. Accordingly, it was demonstrated that the δ nitrogen atom of His, position 3 of the imidazole ring, is frequently involved in a hydrogen bonding with the backbone nitrogen atom of residue $i + 2$, when His is located at the position i of a β-turn[31]. Such a hydrogen bond is observed in Asx-turn and is known to stabilize turn structures.[35] Particularly, a turn involving residues His and Pro at positions i and $i + 1$, respectively, was shown to display two hydrogen bonds, one between C−O(i) and N−H($i + 3$), as observed in β-turn, and a second one connecting the δ His nitrogen to the main chain as described in Asx-turn.[36] Such a complex hydrogen bonding network, observed in Asx-Pro turn, could represent an essential structural feature of the turn-like bioactive conformation of the N-terminal domain of PACAP. This last hypothesis is also consistent with the fact that analogues **31** and **32** behave as weak agonists showing however a relatively high affinity for the PAC1 receptor.

Conclusion

This SAR study focusing on the N-terminal domain of PACAP indicates that Asp^3 and Phe^6 are key elements of the pharmacophore toward the PAC1 receptor. At the opposite, hydroxyl functions of residues Ser^2 and Thr^7 do not participate to the activation of the receptor. The replacement of Phe^6 with bulky aromatic residues produced superagonists of the PAC1 receptor. Moreover, the presence of the C-terminal 28−38 segment seems to influence the binding affinity and the potency of PACAP without affecting the efficacy of the peptide to induce calcium mobilization, as the chemical modifications applied to the N-terminal domain were generally less deleterious to PACAP38 analogues than to PACAP27 derivatives. We have also characterized a new potent PAC1 receptor antagonist,

compound **34**. This latter compound is actually more potent than **81** to block the calcium mobilization induced by PACAP38. This study also indicates that the helical structure observed for residues Ile[5]-Phe[6]-Thr[7], when PACAP27 is bound to DPC-micelles, is essential for the binding of PACAP to the PAC1 receptor. In particular, our results suggest that the N-terminal domain (His[1]-Ser[2]-Asp[3]-Gly[4]) needs to adopt a precise conformation, similar to an Asx-Pro turn, in order to activate the PAC1 receptor. For instance, derivatives such as His(3-Me) and Sar, which are known inhibitors of the hydrogen bonding network observed in Asx-Pro turn,[35,36] produced antagonists or weak partial agonists when incorporated at positions 1 and 4 of the N-terminal segment of PACAP, respectively. In addition, structural investigations carried out with the potent constrained PAC1 agonist, **61**, also suggest a turn-like conformation for residues 1−4. Considering that this N-terminal tail is mainly responsible for the activation of the PAC1 receptor, this tridimensional bioactive structure, inferred from SAR and structural analyses, might constitute an appropriate molecular scaffold supporting the rational design of nonpeptide PAC1 receptor agonists. Because activation of the PAC1 receptor stimulates neuronal survival, the development of potent nonpeptidic agonists represents a critical issue for the development of new therapeutic strategies for the treatment of neurodegenerative diseases.

Experimental Section

Materials. Protected amino acids, Rink-amide AM polystyrene resin, and chemicals for peptide synthesis were purchased from Matrix Innovation (Montreal, Canada), Novabiochem (San Diego, CA), Chem-Impex (Wood Dale, IL), and NeoMPS (San Diego, CA). Trifluoroacetic acid (TFA) was obtained from PSIG (Montreal, Canada). Acetonitrile (ACN), diethylether, *N*,*N*-dimethylformamide (DMF), 1-methyl-2-pyrrolidone (NMP), and dichloromethane (DCM) were obtained from Fisher Scientific (Nepean, Canada). Na[125]I was purchased from Amersham Bioscience (Montreal, Canada). Fluo-4 acetoxymethylester (fluo-4AM) was purchased from Molecular Probes (Leiden, Netherlands). Phospholipids dodecylphosphocholine-d_{38} (DPC-d_{38}) was obtained from C/D/N isotopes (Pointe-Claire, Canada). D_2O and 2,2-dimethyl-2-silapentane-5-sulfonate (DSS) were from Euriso-top (Gif-sur-Yvette, France). All other chemicals were from Sigma Aldrich (Mississauga, Canada).

General Procedure for Solid Phase Peptide Synthesis. All peptides were synthesized using a procedure based on Fmoc chemistry and a BOP (benzotriazol-1-yl-oxy-*tris*(dimethylamino)-phosphonium hexafluorophosphate) coupling strategy. Rink-amide AM-functionalized polystyrene resin was used as the solid support. All Fmoc-amino acids (3 equiv) were coupled using an in situ activation with BOP (3 equiv) and diisopropylethylamine (DIEA, 5 equiv) in DMF/NMP (50/50) for 45 min. Each coupling step was monitored using the ninhydrin test. Coupling of Fmoc-amino acids on secondary amine (following *N*-methyl residues, Pro, Hyp, D-Pro, Ind, Tic, Tiq, or Disc) were repeated until satisfactory coupling yield, evaluated by microcleavage, was obtained. To remove the Fmoc protecting group at every step, 20% piperidine/DMF was used. Cleavage from the resin was achieved with a mixture of TFA/ethanedithiol/phenol/water (92/2.5/3/2.5) for 3 h. After filtration of the resin and subsequent TFA evaporation, crude peptides were precipitated and washed with diethylether before being dried in vacuo.

Peptide Purification and Characterization. All crude peptides were purified by preparative reversed-phase high performance liquid chromatography (RP-HPLC) using a linear gradient of ACN in TFA/H_2O (0.06%, v/v) at a flow rate of 20 mL/min. Preparative RP-HPLC was carried out using a C_{18} (5 μm, 300 Å) column (250 mm × 21.2 mm) connected to a Waters PrepLC500A system equipped with an absorbance detector. Collected fractions were analyzed using analytical RP-HPLC and matrix-assisted laser desorption time-of-flight (MALDI-TOF) mass spectrometry. Analytical RP-HPLC analyses were performed on a Jupiter C_{18} column (5 μm, 300 Å, 250 mm × 4.6 mm) connected to a Beckman 128 pump module coupled to a model 168 PDA detector. The flow rate was maintained at 1 mL/min, and the elution was carried out with a linear gradient of ACN in TFA/H_2O (0.06%, v/v). MALDI-TOF mass spectrometry analyses were performed using a Voyager DE system from Applied Biosystems in linear mode with α-cyano-4-hydroxycinnamic acid as a matrix. Fractions corresponding to the desired product were finally pooled and lyophilized. Analytical RP-HPLC analysis revealed that the purity of all peptides after purification was higher than 95%. A table reporting calculated and obtained by MS-MALDI-TOF molecular weights, as well as the retention times determined by HPLC analyses, is available as Supporting Information.

Binding Assay. Acetyl-PACAP27 was radiolabeled with Na[125]I using the lactoperoxidase procedure.[37] Binding assay was performed using Chinese hamster ovary (CHO) cells stably transfected with the recombinant human PAC1 as previously described.[38] CHO transfected cells express a high PAC1-receptor density of 300 ± 54 fmol/mg protein with a corresponding K_d value of 0.50 ± 0.09 nM with [125]I-Ac-PACAP27 used as a tracer. Briefly, cells were exposed to increasing concentrations of peptides in the presence of 0.1 nM [125]I-Ac-PACAP27. After 90 min of incubation at room temperature, cells were washed and lysed, and the cell-bound radioactivity was quantified using a γ-counter. Results were expressed as a percentage of the specific binding of [125]I-Ac-PACAP27 obtained in the absence of competitive ligands. Nonspecific binding was determined in the presence of 10 μM PACAP38.

Calcium Mobilization Assay. The effect of peptides on Ca^{2+} mobilization was evaluated with a fluorometric imaging plate reader FlexStation II from Molecular Devices (Sunnyvale, CA) as previously detailed.[38] Briefly, CHO cells stably transfected with the recombinant human PAC1 were plated in 96-well plates with black wall and clear bottom 24 h before the assay. After washing, fluo-4 AM dye was added to each well and cells were incubated in the dark for 60 min at 37 °C. Cells were then rinsed and HBSS buffer was added to each well. After a postincubation of 15 min at 37 °C, cells were excited at 480 nm and fluorescence emission was recorded at 525 nm over a 150 s period at 1.52 s intervals. Then, 18 s after the beginning of the reading, peptide solution was added to each well in order to reach assay concentrations ranging from 1×10^{-12} to 1×10^{-5} M. Peptide solutions were previously prepared in 96-well plates in order to reach final concentrations ranging from 5×10^{-12} to 5×10^{-5} M. Results were expressed as a percentage of the response (fluorescence intensity) obtained with 1×10^{-5} M PACAP38 added to each experimental plate. Antagonist assays were performed similarly, except that cells were exposed for 15 min to antagonists before the beginning of the reading. The antagonistic activity of all inactive analogues was first determined by analyzing the capacity of a concentration of 10^{-5} M to reduce the response induced by 10^{-6} M PACAP38. For **34**, **36**, and **66**, which exhibited significant antagonistic properties, the effects of graded concentrations (1×10^{-7} to 1×10^{-5} M) on PACAP38 induced calcium mobilization were tested. To determine pA2 values, a Schild analysis was performed.[26]

NMR Spectroscopy. All NMR experiments were performed on a Brüker Avance DMX 600 NMR spectrometer (Wissembourg, France), equipped with a triple resonance cryoprobe including shielded *z*-gradients. Compounds **1**, **61**, or **65** were dissolved at a concentration of 1 mM in 10% D_2O/H_2O in the presence of 100 mM DPC-d_{38}. DSS was added as an internal ^1H chemical shift reference. The following conventional two-dimensional experiments were carried out: COSY, TOCSY, and NOESY at 298 K. TOCSY experiments were performed with a 80 ms DIPSI2 spin lock mixing pulse. NOESY spectra were collected at mixing times of 100 and 150 ms. Water suppression was achieved by using the excitation sculpting sequence, except for the COSY experiments, where a low power presaturation was applied during the relaxation delay. TOCSY and NOESY experiments were performed in the phase-

sensitive mode, using a proportional phase incrementation method for quadrature detection (States-TPPI). Spectra were collected with 512 and 2048 complex data points in t_1 and t_2 dimensions. Data were processed on Windows workstations, using TOPSPIN software (Brüker, Wissembourg, France). The t_1 dimension was zero-filled to 1024 real data points with the t_1 and t_2 dimensions being multiplied by Gaussian or shifted sinebell functions prior to Fourier transformation. Proton chemical shifts were reported relative to DSS taken as an internal reference. The sequential assignment was performed at 298 K using the standard sequential assignment strategy.[21] ^{1}H chemical shifts of **1**, **61**, and **65** are available in the Supporting Information.

Experimental Restraints. Distance restraints for **1**, **61**, or **65** structure calculations were derived from NOE cross-peaks in the NOESY spectrum recorded with a mixing time of 100 or 150 ms and NOE cross-peaks were integrated into distances by volume integration using the Felix software (Accelrys, France). The NOE volumes were calibrated from geminal Hγ cross-peak of methionine, which corresponds to a distance of 1.8 Å. A range of 25% of the calculated distance was used to define the upper and lower bounds of the restraints.

Structure Calculations. Three-dimensional structures were calculated in vacuo on a Silicon Graphics Indigo2 workstation with the program CNX (Accelrys, France). The target function was similar to that used by Nilges[39] and a force field adapted for NMR structure determination (parallhdg.pro and topallhdg.pro in X-PLOR) was used. A first set of structures was generated, based on the amino acid sequence and on a starting set of distance restraints, using an ab initio simulated annealing protocol. During the whole process, the distance restraint force was kept at 50 kcal Å^{-2} and the NOE intensities were averaged with the "sum" option. Starting from an extended conformation, a first phase of 20 ps dynamics (time step = 2 fs) at 1000 K was followed by 40 ps slow cooling steps to 100 K (time step = 2 fs). A low weight of the van der Waals repulsive term was used at high temperature to allow a large conformation sampling. The variation of the slope of the asymptote in the NOE potential function allowed a progressive fit of the distance restraints. The structures leading to no systematic distance violation larger than 0.2 Å were submitted to further refinement. A 40 ps simulated annealing procedure from 1000 to 100 K (time step = 2 fs) with smoothing of the van der Waals repulsions and square-shaped NOE potential was applied. A final minimization was carried out using the force field derived from CHARMM22 to yield a final set of optimized structures. Analysis of the structures made it possible to resolve ambiguities in the assignment of NOE cross-peaks, which arose from chemical shift degeneracy. This procedure was iterated several times by calculating, at each step, a new set of structures with an improved list of restraints. Nevertheless, some ambiguous assignments still remained and were introduced with an appropriate treatment in CNX. A final set of structures was then generated. The final structures were analyzed by CNX and homemade scripts and displayed by using SYBYL package (Tripos, USA).

Statistical Analysis. Results were mean ± SEM of 3−10 independent experiments. IC_{50}, EC_{50}, and maximal efficacy were calculated using a nonlinear least-squares regression obtained with the Prism 4.0 software. Evaluation of the results was made using the Student's *t*-test and statistical significance was established at $P < 0.05$.

Acknowledgment. This work was supported by the Institut National de la Recherche Scientifique, the Institut National de la Santé et de la Recherche Médicale (INSERM U413), the Conseil Régional de Haute-Normandie, the IREB, the IRME, the ANR, and a scientific exchange program from INSERM and the Fonds de la Recherche en Santé du Québec (FRSQ). Parts of these studies were performed with the support of the Platform for Cell Imaging of Haute-Normandie (PRIMACEN). NMR and molecular modeling software facilities were provided by the Centre de Ressources Informatiques de Haute-Normandie (France). The authors thank Dr. Coadou for structure analysis script disposal and Colas Calbrix for technical support. S.B. is a recipient of a doctoral studentship from the Heart and Stroke Foundation of Canada. H.V. is an affiliated Professor at the Institut National de la Recherche Scientifique—Institut Armand-Frappier.

Supporting Information Available: Tables reporting the retention time detrmined by analyticial HPLC analyses and the calculated and found molecular weight, tables reporting ^{1}H chemical shifts of **1**, **61**, and **65**, figures of the summary of NOE connectivities observed for **1**, **61**, and **65**. This material is available free of charge via the Internet at http://pubs.acs.org.

References

(1) Foord, S. M. Receptor classification: post genome. *Curr. Opin. Pharmacol.* **2002**, *2*, 561–566.
(2) Neer, R. M.; Arnaud, C. D.; Zanchetta, J. R.; Prince, R.; Gaich, G. A.; Reginster, J. Y.; Hodsman, A. B.; Eriksen, E. F.; Ish-Shalom, S.; Genant, H. K.; Wang, O.; Mitlak, B. H. Effect of parathyroid hormone (1−34) on fractures and bone mineral density in postmenopausal women with osteoporosis. *N. Engl. J. Med.* **2001**, *344*, 1434–1441.
(3) Holz, G. G.; Chepurny, O. G. Glucagon-like peptide-1 synthetic analogs: new therapeutic agents for use in the treatment of diabetes mellitus. *Curr. Med. Chem.* **2003**, *10*, 2471–2483.
(4) Olesen, J.; Diener, H. C.; Husstedt, I. W.; Goadsby, P. J.; Hall, D.; Meier, U.; Pollentier, S.; Lesko, L. M. Calcitonin gene-related peptide receptor antagonist BIBN 4096 BS for the acute treatment of migraine. *N. Engl. J. Med.* **2004**, *350*, 1104–1110.
(5) Beebe, X.; Darczak, D.; Davis-Taber, R. A.; Uchic, M. E.; Scott, V. E.; Jarvis, M. F.; Stewart, A. O. Discovery and SAR of hydrazide antagonists of the pituitary adenylate cyclase-activating polypeptide (PACAP) receptor type 1 (PAC1-R). *Bioorg. Med. Chem. Lett.* **2008**, *18*, 2162–2166.
(6) Petersen, K. F.; Sullivan, J. T. Effects of a novel glucagon receptor antagonist (Bay 27-9955) on glucagon-stimulated glucose production in humans. *Diabetologia* **2001**, *44*, 2018–2024.
(7) Hoare, S. R. Mechanisms of peptide and nonpeptide ligand binding to Class B G-protein-coupled receptors. *Drug Discovery Today* **2005**, *10*, 417–427.
(8) Gefel, D.; Hendrick, G. K.; Mojsov, S.; Habener, J.; Weir, G. C. Glucagon-like peptide-I analogs: effects on insulin secretion and adenosine 3′,5′-monophosphate formation. *Endocrinology* **1990**, *126*, 2164–2168.
(9) Dennis, T.; Fournier, A.; Cadieux, A.; Pomerleau, F.; Jolicoeur, F. B.; St Pierre, S.; Quirion, R. hCGRP8-37, a calcitonin gene-related peptide antagonist revealing calcitonin gene-related peptide receptor heterogeneity in brain and periphery. *J Pharmacol. Exp. Ther.* **1990**, *254*, 123–128.
(10) Robberecht, P.; Gourlet, P.; De Neef, P.; Woussen-Colle, M. C.; Vandermeers-Piret, M. C.; Vandermeers, A.; Christophe, J. Receptor occupancy and adenylate cyclase activation in AR 4-2J rat pancreatic acinar cell membranes by analogs of pituitary adenylate cyclase-activating peptides amino-terminally shortened or modified at position 1, 2, 3, 20, or 21. *Mol. Pharmacol.* **1992**, *42*, 347–355.
(11) Neumann, J. M.; Couvineau, A.; Murail, S.; Lacapère, J. J.; Jamin, N.; Laburthe, M. Class-B GPCR activation: is ligand helix-capping the key? *Trends Biochem. Sci.* **2008**, *33*, 314–319.
(12) Ohtaki, H.; Nakamachi, T.; Dohi, K.; Aizawa, Y.; Takaki, A.; Hodoyama, K.; Yofu, S.; Hashimoto, H.; Shintani, N.; Baba, A.; Kopf, M.; Iwakura, Y.; Matsuda, K.; Arimura, A.; Shioda, S. Pituitary adenylate cyclase-activating polypeptide (PACAP) decreases ischemic neuronal cell death in association with IL-6. *Proc. Natl. Acad. Sci. U.S.A.* **2006**, *103*, 7488–7493.
(13) Vaudry, D.; Rousselle, C.; Basille, M.; Falluel-Morel, A.; Pamantung, T. F.; Fontaine, M.; Fournier, A.; Vaudry, H.; Gonzalez, B. J. Pituitary adenylate cyclase-activating polypeptide protects rat cerebellar granule neurons against ethanol-induced apoptotic cell death. *Proc. Natl. Acad. Sci. U.S.A.* **2002**, *99*, 6398–6403.
(14) Aubert, N.; Vaudry, D.; Falluel-Morel, A.; Desfeux, A.; Fisch, C.; Ancian, P.; de Jouffrey, S.; Le Bigot, J. F.; Couvineau, A.; Laburthe, M.; Fournier, A.; Laudenbach, V.; Vaudry, H.; Gonzalez, B. J. PACAP prevents toxicity induced by cisplatin in rat and primate neurons but not in proliferating ovary cells: involvement of the mitochondrial apoptotic pathway. *Neurobiol. Dis.* **2008**, *32*, 66–80.
(15) Dejda, A.; Jolivel, V.; Bourgault, S.; Seaborn, T.; Fournier, A.; Vaudry, H.; Vaudry, D. Inhibitory effect of PACAP on caspase activity in neuronal apoptosis: A better understanding towards a therapeutic potential in neurodegenerative diseases. *J. Mol. Neurol.* **2008**, *36*, 26–37.

(16) Vaudry, D.; Gonzalez, B. J.; Basille, M.; Yon, L.; Fournier, A.; Vaudry, H. Pituitary adenylate cyclase-activating polypeptide and its receptors: from structure to functions. *Pharmacol. Rev.* **2000**, *52*, 269–324.
(17) Bourgault, S.; Vaudry, D.; Guilhaudis, L.; Raoult, E.; Couvineau, A.; Laburthe, M.; Ségalas-Milazzo, I.; Vaudry, H.; Fournier, A. Biological and Structural Analysis of Truncated Analogs of PACAP27. *J. Mol. Neurosci.* **2008**, *36*, 260–269.
(18) Inooka, H.; Ohtaki, T.; Kitahara, O.; Ikegami, T.; Endo, S.; Kitada, C.; Ogi, K.; Onda, H.; Fujino, M.; Shirakawa, M. Conformation of a peptide ligand bound to its G-protein coupled receptor. *Nat. Struct. Biol.* **2001**, *8*, 161–165.
(19) Sun, C.; Song, D.; Davis-Taber, R. A.; Barrett, L. W.; Scott, V. E.; Richardson, P. L.; Pereda-Lopez, A.; Uchic, M. E.; Solomon, L. R.; Lake, M. R.; Walter, K. A.; Hajduk, P. J.; Olejniczak, E. T. Solution structure and mutational analysis of pituitary adenylate cyclase-activating polypeptide binding to the extracellular domain of PAC1-RS. *Proc. Natl. Acad. Sci. U.S.A.* **2007**, *104*, 7875–7880.
(20) Sherwood, N. M.; Krueckl, S. L.; McRory, J. E. The origin and function of the pituitary adenylate cyclase-activating polypeptide (PACAP)/glucagon superfamily. *Endocr. Rev.* **2000**, *21*, 619–670.
(21) Wüthrich K. *NMR of Proteins and Nucleic Acids*; Wiley: New York, 1986.
(22) Hruby, V. J. Designing peptide receptor agonists and antagonists. *Nat. Rev. Drug Discovery* **2002**, *1*, 847–858.
(23) Chatterjee, J.; Gilon, C.; Hoffman, A.; Kessler, H. *N*-Methylation of peptides: a new perspective in medicinal chemistry. *Acc. Chem. Res.* **2008**, *41*, 1331–1342.
(24) Hou, X.; Vandermeers, A.; Gourlet, P.; Vandermeers-Piret, M. C.; Robberecht, P. Structural requirements for the occupancy of rat brain PACAP receptors and adenylate cyclase activation. *Neuropharmacology* **1994**, *33*, 1189–1195.
(25) Freidinger, R. M. Design and synthesis of novel bioactive peptides and peptidomimetics. *J. Med. Chem.* **2003**, *46*, 5553–5566.
(26) Arunlakshana, O.; Schild, H. O. Some quantitative uses of drug antagonists. *Br. J. Pharmacol. Chemother.* **1959**, *14*, 48–58.
(27) Robberecht, P.; Gourlet, P.; De Neef, P.; Woussen-Colle, M. C.; Vandermeers-Piret, M. C.; Vandermeers, A.; Christophe, J. Structural requirements for the occupancy of pituitary adenylate-cyclase-activating-peptide (PACAP) receptors and adenylate cyclase activation in human neuroblastoma NB-OK-1 cell membranes. Discovery of PACAP(6−38) as a potent antagonist. *Eur. J. Biochem.* **1992**, *207*, 239–246.
(28) Wray, V.; Kakoschke, C.; Bokhara, K.; Naruse, S. Solution structure of pituitary adenylate cyclase activating polypeptide by nuclear magnetic resonance spectroscopy. *Biochemistry* **1993**, *32*, 5832–5841.
(29) Wilmot, C. M.; Thornton, J. M. Analysis and prediction of the different types of beta-turn in proteins. *J. Mol. Biol.* **1988**, *203*, 221–232.
(30) Chou, P. Y.; Fasman, G. D. Prediction of protein conformation. *Biochemistry* **1974**, *13*, 222–245.
(31) Hutchinson, E. G.; Thornton, J. M. A revised set of potentials for beta-turn formation in proteins. *Protein Sci.* **1994**, *3*, 2207–2216.
(32) Moehle, K.; Gussmann, M.; Hofmann, H. J. Structural and energetic relations between β-turns. *J. Comput. Chem.* **1997**, *18*, 1415–1430.
(33) Cann, J. R.; London, R. E.; Unkefer, C. J.; Vavrek, R. J.; Stewart, J. M. CD-NMR study of the solution conformation of bradykinin analogs containing alpha-aminoisobutyric acid. *Int. J. Pept. Protein Res.* **1987**, *29*, 486–496.
(34) Lang, M.; De Pol, S.; Baldauf, C.; Hofmann, H. J.; Reiser, O.; Beck-Sickinger, A. G. Identification of the key residue of calcitonin gene related peptide (CGRP) 27−37 to obtain antagonists with picomolar affinity at the CGRP receptor. *J. Med. Chem.* **2006**, *49*, 616–624.
(35) Abbadi, A.; Mcharfi, M.; Aubry, A.; Premilat, S.; Boussard, G.; Marraud, M. Involvement of side functions in peptide structures: the Asx turn. Occurrence and conformational aspects. *J. Am. Chem. Soc.* **1991**, *113*, 2729–2735.
(36) Blank, J. T.; Guerin, D. J.; Miller, S. J. A His-Pro-Aib peptide that exhibits an Asx-Pro-turn-like structure. *Org. Lett.* **2000**, *2*, 1247–1249.
(37) Vaudry, D.; Hamelink, C.; Damadzic, R.; Eskay, R. L.; Gonzalez, B.; Eiden, L. E. Endogenous PACAP acts as a stress response peptide to protect cerebellar neurons from ethanol or oxidative insult. *Peptides* **2005**, *26*, 2518–2524.
(38) Bourgault, S.; Vaudry, D.; Botia, B.; Couvineau, A.; Laburthe, M.; Vaudry, H.; Fournier, A. Novel stable PACAP analogs with potent activity towards the PAC1 receptor. *Peptides* **2008**, *29*, 919–932.
(39) Nilges, M. Calculation of protein structures with ambiguous distance restraints. Automated assignment of ambiguous NOE crosspeaks and disulphide connectivities. *J. Mol. Biol.* **1995**, *245*, 645–660.

JM900291J